Evaluation of precipitation over the Middle East and Mediterranean in high resolution climate models

Abstract

The Middle East is considered the worlds most water scarce region (Brown & Crawford (2009)). In this study two high resolution climate models have been evaluated to compare how successfully they model precipitation over the region. One model is HiGEM (Sha rey et al. (2009)), a global coupled

Two regions have been defined for statistical analysis and bias, root mean square error and pattern correlations have been calculated for each. The e ect of smoothing precipitation fields on statistics has been investigated. This investigation has been furthered by calculating fractions skill score curves, a novel method implemented recently for numerical weather prediction (Roberts & Lean (2008)). This method is new for climate analysis and comments on the usefulness of the method have been made, along with recommendations for future use.

Acknowledgements

There are many people that I owe a debt of gratitude to academically and non-academically - too many to name here. Thanks go to Len and Emily, who gave me everything I needed from my supervisors, and more.

Thanks go to my parents - Dad for showing me that nothing is broken which can't be fixed, and Mum for reminding me what's important when my head gets filled up with big ideas.

I gratefully acknowledge NERC for their financial support, without which I would have been unable to undertake this course.

Last but not least I thank my coursemates at Reading, who have been a big part in making this year one of my best so far. Writing this dissertation was (almost) a breeze with the company in room 105. Having others to share the tea-making burden with helped me get through some of the harder bits - sorry if I drank more than I made!

To those who do not know mathematics it is di cult to get across a real feeling as to the beauty, the deepest beauty, of nature ... If you want to learn about nature, to appreciate nature, it is necessary to understand the language that she speaks in. **- Richard Feynman**

I confirm that this is my own work and the use of all material from other sources has been properly and fully acknowledged.

. . . . . .

. . . . . .

List of Figures

Contents

region which will be addressed in this study are also set out.

1.1 Geography

A map of the Middle East is shown in figure 1.1. The region has a var

dan is used for human purposes, which has caused a large reduction in flow of the river. Coupled with the high evaporation rate, this means that the Dead sea is drying up (Klein & Flohn (1987)).

The two other major rivers in the region are the Tigris and the Euphrates, which descend from the slopes of the Taurus moune ins in Turkey into Syria and Iraq before discharging into the Persian Gulf. These rivers define Mesopotamia, also known as the "'Cradle of Civilization'. This area saw the development of some of the earliest human civilizations, in no small part due to its rich, fertile soils – hence the name 'The Fertile Crescent'. It has now all but dried up, with much of the land cover transformed into bare land and salt crust, and it is on the WWF list of critical/endangered ecoregions (Olson & Dinerstein (2002)). Human activity is a major factor behind this degradation – water diversion for agricultural irrigation and construction of many dams in the headwaters of the Tigris and Euphrates have caused a reduction in their annual flow (Partow (2001)). This combination of stress on a fresh water source and rapid population growth substantially increases the vulnerability of the region to future climate change (Evans (2008)).

1.2 Climate

The Middle East has a Mediterranean macroclimate, characterized by cool, wet winters and hot, dry summers. Nearly all precipitation falls in winter, the dominant mechanism being eastward moving cyclones from the Mediter-

- The Zagros mountains of Iran.
- The Pontic range by the Black Sea.
- The Elburz range by the Caspian Sea.

Precipitation patterns are also influenced by the location of water bodies adjacent to the mountains. The Black and Caspian Seas, and eastern coast of the Mediterranean act as water sources for orographic precipitation. The Red Sea and Persian Gulf act as powerful sources of water vapour, however they trigger little precipitation locally due to the descending air in the Hadley cell (Evans (2004)). Water bodies are also a source of sea–breeze related precipitation, whereby unequal heating of land and sea generates a pressure di erence which produces a wind component moving toward the land during the day, bringing with it moisture from the sea.

The mountains have a further indirect e ect on precipitation. Through elevated heating they generate atmospheric subsidence that warms and dries the surrounding areas (Broccoli & Manabe (1992)), and it has been shown that summer subsidence forced by the Iranian Plateau adds extra warming and drying to Mesopotamia (Evans (2004)). This drying of surrounding areas partially explains the existence of deserts in the region. The desertification of the region can also be attributed to remote larger-scale climate behaviour such as the 'monsoon-desert mechanism' (Rodwell & Hoskins (1996)), in which diabatic heating in the Asian monsoon region induces a Rossby-wave pattern to the west which acts in combination with descending air in the Hadley cell to inhibit precipitation in the region. This is a factor behind the extremely dry summer climate, as the Asian monsoon peaks during this period (Rodwell & Hoskins (1996)).

There is a high temporal as well as spatial variability in rainfall in the Middle East. There is day to day variability in winter due to individual storms passing through the region. There is also the large annual variability from its

Figure 1.2: ***Temperature and precipitation changes over Europe and the Mediterranean from A1B (high emission) simulations. Top row: Annual mean, DJF and JJA temperature change between 1980 to 1999 and 2080 to 2099, averaged over 21 models. Middle row: same as top, but for fractional change in precipitation. Bottom row: number of models out of 21 that project increases in precipitation (Christensen et al. (2007))***

dwindling resource. This study focuses on precipitation in climate models and specifically how the current trend toward higher spatial resolution will improve the accuracy of precipitation predictions. The questions upon which this study focus are laid out in the next section.

1.4 Aims of the study

There are many conceptual models of the climate, ranging from simple radia-

- To investigate how the variation of model skill with resolution might be represented

In the next chapter the theory and basic ideas behind climate modeling are discussed, along with a more complete description of the two models used in this study as well as the observations used for comparison.

Chapter 2

Model description and observations

Climate models have varying levels of complexity, ranging from simple radiation budget models, through to basic atmosphere only models to Earth system models which include components for the ocean, the cryosphere, the biosphere and more. They are widely used to understand and predict the evolution of the climate and have recently been the key to attributing recent change in climate to human activities (Slingo et al. (2009)). Before climate models are used for prediction however, they must be validated against past observations to verify that they are representing the climate system accurately.

The focus of this chapter is climate modelling and the di erent types of models used. The importance of model resolution for the representation of climate is discussed. Finally the two models used in this study are described, as well as the di erent observational datasets used for validation against the models.

2.1 Climate Modelling

A climate model is an attempt to represent the many processes that produce climate in a mathematical model. The aim is to understand these processes

figure 2.1, along with the topography as it is represented by the two models used in this study.

Whilst the move towards higher resolution goes on (some atmosphere-only models now operate at resolutions of 20km (Kitoh et al. (2008))), it may be that the cost of the extra computing power will outweigh the increase of skill gained by moving to higher resolutions. In NWP this is especially a problem since a move to smaller scales results in forecast errors growing more rapidly, and so higher resolution many not give any significant increase in model skill (Lorenz (1969), Done et al. (n.d.), Mass et al. (2002)). Because of

934(e)0.0490113(

	HiGEM	Regional Model
Region	Whole globe	Europe, Mediterranean & Middle East
Components	Coupled atmosphere and ocean	Atmosphere only
Resolution	1.25° x 0.83° for atmosphere 1/3° x 1/3° for the ocean	0.44° x 0.44°
Vertical levels	38 in atmosphere, 40 in the ocean	19
Lateral boundary conditions	None needed	From HadAM3P

Table 2.1: ***Comparison of the two models used in this study.***

the equator) in the ocean. In HiGEM this has been increased to 1.25° x 0.83° in longitude and latitude for the atmosphere, and 1/3° x 1/3° globally for the ocean and sea ice. The timestep of the model is 20 minutes (Sha rey et al. (2009)).

is shown in figure 2.1.

Climatologies are based on years 21–70 of a model run, so that the upper ocean and atmosphere have su cient time to spin up. Initial conditions have been given to the model to simulate climate over the past half century.

2.2.2 The Regional Climate Model

The RCM used in this study is based on PRECIS, a model based on HadAM3P, a global, atmosphere-only model developed at the Hadley Centre. The RCM has a horizontal resolution of 0.44°, giving a grid spacing of 50km. This permits a large domain to be used whilst representing significantly more topographic variation than is possible in the 200km scale of the generation of climate models used in IPCC (Black (2009), Slingo et al. (2009)) (topography as represented by the RCM is shown in figure 2.1). The model has 19 levels in the vertical and includes the whole Mediterranean so that cyclones which bring most of the rain to the Middle East do not travel through the domain boundary (Black (2009)). The domain of the model is shown in figure 2.2. It should be noted that there are normally problems associated with model output close to the boundary, therefore when the RCM will be evaluated only output at some distance from the boundary will be looked at.

RCMs are applied over a limited area and so require input at both the surface and lateral boundaries of the domain. Lateral boundary conditions were derived from integrations of HadAM3P forced with surface boundary conditions (sea surface temperature, sea ice fraction), which were derived from observations. Boundary conditions for the PRECIS RCM are on a grid of 2.5° latitude x 3.75° longitude, about 300 km resolution at 45N or 400 km at the equator. Surface boundary conditions for the RCM are based on HadCM3 predictions and observations (Black (2009)).

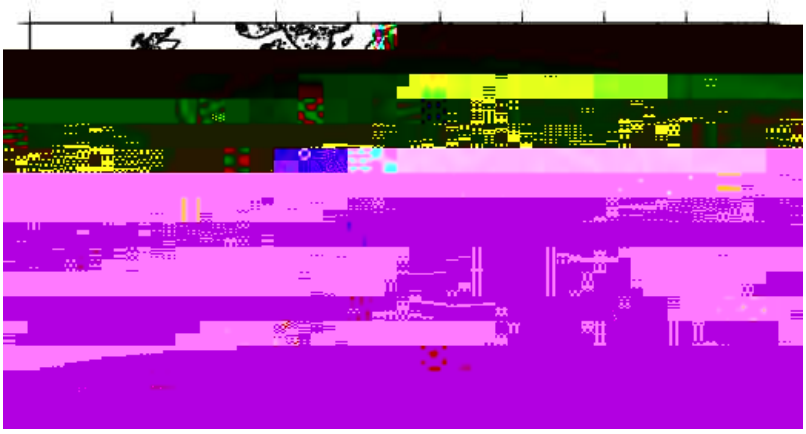

Figure 2.2: *The domain over which the regional model is evaluated.*

2.3 Description of observations

Compared with many places in the world, the Middle East is a data sparse area (Evans (2004)). As such, several di erent observational datasets, each with their own advantages and disadvantages, have been used.

The global precipitation dataset from the global precipitation climatology centre (GPCC) is used. This data is based upon quality controlled ground station data from up to 43,000 stations, with irregular coverage in time. These provide a 1° x 1° resolution precipitation climatology for the period 1951 to 2004 (Earth System Research Laboratory (2009)).

Global precipitation climatology project (GPCP) data are also used. This consists of data from over 6,000 rain gauge stations, satellite geostationary and low-orbit infrared, passive microwave, and sounding observations which are merged to estimate monthly rainfall on a 2.5° global grid from 1979 to

lated from 1997 to 2007 and consist of TRMM observations constrained with gauge station and GPCP data (Hu man, G.J. and Adler, R.L. and Bolvin, D.T. and Gu, G. and Nelkin, E.J. and Bowman, K.P. and Hong, Y. and Stocker, E.F. and Wol , D.B. (2007)).

To compare mean sea level pressure and wind fields in the models, data from ERA-40 reanalysis was used. ERA reanalysis is a dataset created by assimilating many sources of observations into the ECMWF climate model at a 40km resolution (Uppala et al. (2005)).

Chapter 3

Visual comparison of climatologies

HiGEM and the Regional Climate Model have been run to produce climatologies over the Middle East. These climatologies give average values of meteorological variables for the domains over which they are run. Although the focus of this study is specifically to investigate how well the models represent precipitation, it is important to evaluate how well the models represent other aspects of the climate system. This is because there are di erent climatological processes that cause precipitation and so how a model represents precipitation is dependent on how well it represents these processes, which are dependent on other meteorological variables.

In this chapter model climatologies for precipitation, 10m surface wind fields and mean sea level pressure are plotted and visually compared to climatologies taken from a variety of observations. Several observational datasets for precipitation have been plotted which have their own adv

3.1 Precipitation

3.1.1 Comparing observations

Shown in figure 3.1 are observed precipitation climatologies. (a) and (b) show boreal winter (DJF) and summer (JJA) observations from the GPCC dataset (Earth System Research Laboratory (2009)). White areas are shown over land because the data is taken from rain gauge and gauge station data and no data is available over the sea. Shown in (c) and (d) are DJF and JJA climatologies taken from the GPCP dataset (NASA Goddard Space Flight Center (2009)) - the dataset based on gauge station, satellite and

and can be seen from rainfall gauge data (Sharon & Kutiel (1986), Black (2009)). In particular it falls along the length of the Jordan river, upon which many communities depend heavily. Moving eastward from the Mediterranean across Israel and towards the desert there is a sharp gradient in rainfall contour lines, which is almost totally absent in the GPCP data. It is for this reason, along with the fact that GPCP has the lowest resolution of all observations, that the GPCP data will not be used for statistical comparison with the models – attempting to verify a model against observations is a misleading exercise if the observations do not match reality in important areas. The GPCC and TRMM datasets show generally the same pattern of precipitation – they both show the rainfall falling near the Jordan river, they both capture the orographic precipitation in Taurus mountains of South Eastern Turkey where the Euphrates and Tigris begin their journey toward the Persian Gulf and they both capture the wintertime rainfall over the Fertile Crescent.

The GPCC dataset however does not have data over the seas since it comes only from ground stations. It also has a lower resolution than TRMM, which shows a more detailed pattern of precipitation. Conversely, the TRMM climatology is calculated over the shortest time period (1997–2007) whereas the GPCC and GPCP data stretch back over longer time periods (starting from 1951 and 1979 respectively). It is thought however that when it comes to statistical analysis, the advantages of TRMM over the other datasets outweigh the disadvantage of having been calculated over a shorter time period. The TRMM data will therefore be used for model validation.

3.1.2 Looking at the models

Shown in figure 3.2 are precipitation climatologies for the models. (a) and (b) show DJF and summer JJA climatolgoies calculated by HiGEM. (c) and (d) show DJF and JJA climatologies calculated by the RCM. HiGEM fields

are smoother than the RCM due to the lower resolution of the model and

the Mediterranean, bringing wintertime rainfall.

In summer the pressure drops, and the pattern observed is a region of low pressure eastwards towards the Persian Gulf, which increases rapidly northwards and westwards creating a high gradient of pressure associated with high wind speeds through geostrophic balance. A long tongue of low pressure can also be seen in summer, extending westwards from Northern Iraq towards Cyprus and over the Mediterranean. HiGEM pressure fields are shown in 3.3(c) and 3.3(d). It captures the pressure patterns fairly well; the general pattern of high–lowf low

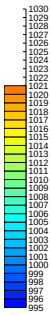
1030
1029
1028
1027
1026
1025
1024
1023
1022
1021
1020
1019
1018
1017
1016
1015
1014
1013
1012
1011
1010
1009
1008
1007
1006
1005
1004
1003
1002
1001
1000
999
998
997
996
995

3.3 Surface Wind Patterns

3.3.1 Observed Wind Fields

Shown in figure 3.4 are climatological 10m surface wind patterns from observations and from models. The observations for DJF and JJA are from ERA-40 reanalysis and are shown in (a) and (b).

The observed winter wind field show relatively low speeds over the much of the land of the Middle East. Strong westerly winds can be seen over the Mediterranean. This is the Mediterranean storm track. Where this meets the land there is slight north easterly flow, which, upon meeting the moist air from the Mediterranean generates convergence and ascent. Since this air holds moisture from passing over the sea, precipitation results, which is observed in this general area. Relatively strong northerly winds are also observed over the Aegean. Winds are generally stronger since the sea surface is generally smoother than the rougher land surface, so winds passing over the sea experience less friction.

The wind patterns are also consistent with the pressure patterns, with wind moving counter-clockwise around the Cyprus low in winter. This can be seen in the westerly Mediterranean storm track and also in the south westerly movement of air over the land to the east of the Mediterranean. There is no corresponding easterly flow to the north however, this could possibly be due to the presence of the Taurus mountains which would hinder any horizontal movement of air.

In summer the wind also follows the pressure patterns, moving counter-clockwise around the strong low pressure area, with greater speeds due to the stronger presssure gradient. Winds over the Mediterranean also have more of a northerly component than in winter. Furthermore, over Turkey the winds are northerly, whereas in winter there is no net wind.

There is also very strong northerly flow over north east Africa in summer;

Chapter 4

Statistical verification methods

The output from the two models has been compared visually with observations and qualitative distinctions have been drawn. Quantitative measures of di erences between models and reality can be obtained by using statistical measures of skill. In this chapter several standard measures are described - the bias, the root mean square error and the pattern correlation. A new method for evaluating how model skill varies with spatial scale is also described. This has been adapted for climate modelling from a new method recently implemented by Roberts and Lean for numerical weather prediction (Roberts & Lean (2008)).

4.1 Statistical measures of model skill

Bias has been used to evaluate model performance against observations, it is calculated as

$$\text{Bias} = \overline{M} - \overline{O} \tag{4.1}$$

where $\overline{M}$ is the spatial mean of a modelled value over a domain and $\overline{O}$ is the spatial mean of observed values. This measures the amount by which

4.2. FRACTIONS SKILL SCORES

$$O(n)(i,j) = \frac{1}{n^2} \sum_{k=1}^{n} \sum_{l=1}^{n} I_0 \left[i + k \right.$$

4.2.3 Computing fractions skill scores

The mean square error (MSE) for the observed and forecast fractions for a neighbourhood of length n is given by

$$MSE_{(n)} = \frac{1}{N_x N_y} \sum_{i=1}^{n} \sum_{j=1}^{n} [O_{(n)i,j}^{(n)}$$

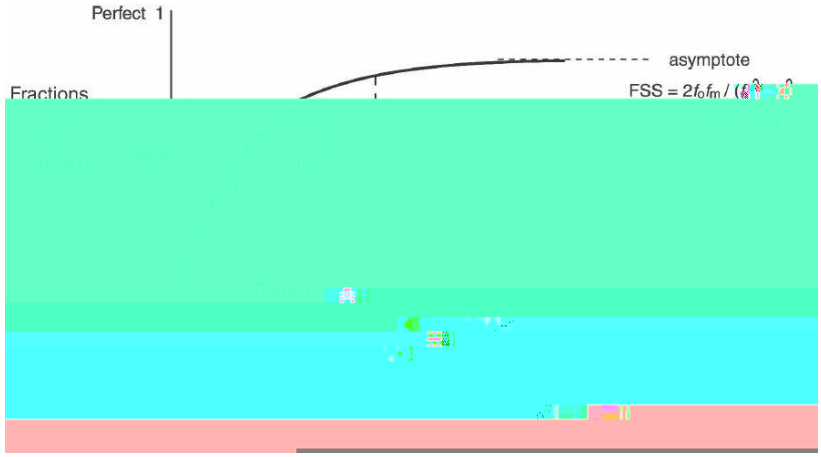

Figure 4.2: ***A schematic graph of FSS against spatial scale, from Roberts & Lean (2008).***

bias then the observed frequency f_O (fraction of observed points exceeding the threshold over the domain) is not equal to the model-forecast frequency f_M, and from equations (4.6), (4.7) and (4.8) it can be shown that

$$AFSS = 1 - \frac{(f_O - f_M)^2}{f_O^2 + f_M^2} = \frac{2f_O f_M}{f_O^2 + f_M^2}, \tag{4.9}$$

Chapter 5

Statistics of model output

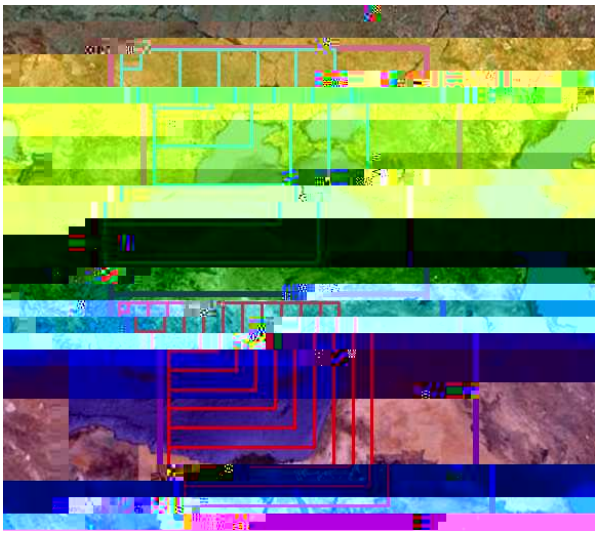

Figure 5.1: *Schematic showing the 'North' region (covering 39–50°N and 26-42°E) and the 'South' region (28–39°N and 26-42°E). Statistics for the whole of each region are discussed in section 5.1. Blue squares show the increasing spatial scales used to calculate HiGEM FSS curves, red squares show those areas used calculating RCM FSS curves (see section 5.2).*

	Bias (mm day^{-1})		RMSE (mm day^{-1}		P. Corr., ρ	
Season - Region	HiGEM	RCM	HiGEM	RCM	HiGEM	RCM
DJF - North	0.03	-0.46	1.00	0.90	0.62	0.65
JJA - North	-0.30					

	Bias (mm day^{-1})		RMSE (mm day^{-1})		P. Corr., ρ	
Season - Region	HiGEM	RCM	HiGEM	RCM	HiGEM	RCM
DJF - North	0.03	-0.47	0.70	0.67	0.75	0.77
JJA - North	-0.29	-0.69	0.58	0.86	0.71	0.71
DJF - South	0.33	-0.46	0.81	0.67	0.91	0.93
JJA - South	0.26	0.13	0.37	0.18	0.93	0.86

Table 5.2: ***Statistical evaluation of precipitation fields over the two regions after one application of the convolution kernel.***

essential for accurate predictions about the hydrology in the region.

The fields were then smoothed by applying the convolution kernel. Which is equivalent to replacing the value at each grid box by a 3 x 3 grid box centred it. The same statistics were then calculated and results are shown in table 5.2.3728(16467(n).218509057(i).042550263)-367.687(t)-0.155063

The first thing to notice is that all bias scores remain the 3.044386(b)-0.312447(i)0.

north region in summer. This can be at least partly attributed to the fairly uniform nature of the fields; smoothing them would not significantly change the pattern they show.

5.2 Fractions Skill Scores.

The fields were bias corrected to remove some of the e ect of bias on mean square error, and fractions skill scores, described in section 4.2, were calculated for both seasons for both models. Scores were calculated for increasing spatial scales (shown in figure 5.1) for each model. These were calculated for both the north and south regions. Curves of FSS against spatial scale are shown in figures 5.2 and 5.3. Di erent thresholds were used in calculating the binary fields, $q \geq 0.5$, 1, 2 and 4mm day^{-1}, these correspond to (a) & (b), (c) & (d), (e) & (f) and (g) & (h) respectively for both figures 5.2 and 5.3.

It can be seen that using a lower threshold gives higher FSS scores for all spatial scales. Furthermore, using a threshold that is greater than the maximum in the field gives undefined values (since the denominator in calculating FSS, MSE_{ref}, becomes zero - see equations 4.7 and 4.8). This is observed in 5.2(h), 5.3(f) and 5.3(h), where the contour lines for the corresponding thresholds lie outside the respective domains in the precipitation fields.

For the lowest thresholds, the FSS start very close to and remain at 1. This is because the threshold is too low and has eliminated information in the field; since nearly all points will lie above the threshold, the binary fields become almost uniform 1's, which tells us nothing about the accuracy of the model.

Increasing the spatial scale through application of the convolution kernel increases the FSS skill score. This shows that the skill is lowest at the grid scale. As the scale increases the FSS asymptotes - the curve can be defined

by the rate at which it does. A curve which increases quickly at first, such as the ones in figures 5.2(g) and 5.3(b), indicates an error which can partly eliminated by looking at a slightly larger scale. This kind of curve would be expected in a case where a model predicted a precipitation field which was slightly o set from observations.

A curve such as the one in 5.3(d), which begins at zero, indicates that at the grid scale the error is the maximum it can be and none of the 1s in the binary field of the model match the 1's in the observations. The scale where the curve increases gives a measure of the skill of the model as well, the larger the scale at which it asymptotes, the bigger the di erence between the model and reality.

Most curves do not asymptote to 1, as they would if they had no bias. Even though the fields have been bias corrected, this means that there is still a remnant bias in the binary fields, since the numbers of 1's in the model fields will not necessarily be equal to the number of 1's in the observed field. This e ect of bias could be totally removed if percentile thresholds were used to create the binary fields, then both the model and observed fields would necessarily have the same frequency of 1's.

FSS curves have a potential usefulness in giving an objective measure to

These are just ideas of how FSS curves may be utilised; curves presented in figures 5.2 and 5.3 are largely a ected by biases and the choice of thresholds - no solid conclusions can be drawn from them before these issues are resolved. The choice of target skill is something which would require further investigation also, di erent users of model output have di erent requirements and some may need much greater skill than others. The approach should be to ask what is required of the output - at what scale are predictions required. For instance, if a general trend in precipitation is needed then the FSS curve would show that a high spatial scale would give a skilful prediction. If however precipitation data on the grid scale is needed then FSS curves show that skill may be lower than is acceptable on this scale and choosing the resolution of model output to use in a study may be a trade-o bethudp63371(f)-327.155(h)-0.310d [(h)-0.310

Chapter 6

Discussion and Conclusions

The Middle East is a semi-arid region which experiences wet winters and dry summers. Rainfall in winter comes mainly from depressions moving eastward from across the Mediterranean. In this study, two climate models, HiGEM, a 1.875° x 1.25° resolution coupled atmosphere-ocean GCM and a 0.44° x 0.44° resolution regional atmosphere-only model have been used to model the climate over the Middle East. The representation of precipitation in the models has been investigated.

Winter and summer climatologies have been compared between the two models and observations, both visually and statistically for precipitation as well other key meteorological variables. Precipitation bias, root mean square error (RMSE) and pattern correlation have been calculated for two key regions; a region encompassing the Black Sea and northern Turkey, and another encompassing southern Turkey, the Fertile Crescent and areas containing large portions of the drainage basins of the Tigris, Euphrates and Jordan.

Finally a novel method developed recently for NWP (Roberts & Lean (2008)) for examining the variation of model skill with spatial scale using thresholds has been implemented for the climatologies. Curves of fractions skill score (FSS) against horizontal scale have been plotted for both regions

using di erent thresholds, their shapes and what they can tell us about model performance has been discussed.

6.1 Model Evaluation

Both models represent the seasonal cycle of precipitation well, and show relatively high pattern correlations. However, HiGEM shows a slight positive bias for precipitation and the RCM shows a large negative bias. The conclusion that because the RCM has a large negative bias it is worse than HiGEM is di cult to draw however, due to error compensation. A large negative bias in the RCM could be due to an error from one problem with the model. However HiGEM could potentially have the same problem, yet have an additional problem which overestimates the precipitation; causing the biases from each problem to cancel out. It is important then to bear in mind that looking at precipitation bias alone is insu cient to draw any certain conclusions regarding model performance.

Both models underestimate the magnitude of the winds making up the Mediterranean storm track and have some problems with the region of wintertime low pressure over Cyprus. This is known as the Cyprus low and is associated with wintertime depressions moving eastwards across the Mediterranean. In HiGEM the intensity of the low is underestimated and in the RCM it is almost absent. This would have an e ect on the precipitation in the Middle East; a weaker low would bring fewer weather systems to the region. The major underestimation of the Cyprus low in the RCM is likely to be a factor associated with its large negative precipitation bias.

Both models have errors in surface wind fields around the main region of precipitation around the east coast of the Mediterranean. HiGEM overestimates the convergence in the region and the RCM underestimates it.

tra convergence in HiGEM would give extra ascent and so give too much precipitation, and a lack of convergence in the RCM would give less ascent and so less precipitation. The RCM also has much larger errors in circulation which suggests that errors in precipitation are due to errors in model physics. However all meteorological variables are functions of each other - an error in winds leads to errors in convergence, leading to errors in precipitation. This can alter the radiation reaching the earth and so alter temperature, which in

use of high resolution models pointless.

be to test two models at the same resolution with di erent components. For instance HiGEM could be evaluated against HiGAM, a model which operates at the same resolution as HiGEM but does not contain an ocean. The e ect of resolution on model output could also be tested, for instance if the RCM were run at the lower HiGEM resolution as well the higher resolution.

In this study only multi year climatologies have been compared. Whilst this is a vital part of model performance, it is not the only part. Temporal variability is an aspect of the climate which has not been addressed and would be a mistake to think that good performance in spatial dimensions alone is enough for a model. A model could perform perfectly in predicting the location and magnitude of yearly averages of precipitation, however if it fails to capture temporal variability then it certainly has problems. Thus, more testing of these models should focus on the representation of temporal variability.

Another aspect of the climate which the models should be tested for is representation of extremes. In a region which has already been shown to be at risk from climate change, it is important to be able to predict with accuracy not just how much average amounts of rainfall will change, but how much the frequency of extremes will change, i.e. how often droughts and floods will occur compared to the past. One possible method of analysing extremes would be to look at quantiles; dividing model and observational data into subsets and comparing the highest and lowest sets.

The climate is intrinsically linked to the existence of human civilization and climate change is one of the biggest threats we currently face as a species. Climate models are our best chance at knowing what we can expect from the future. They can make predictions with varying levels of certainty and the drive towards better representation of climate will only improve these predictions. By validating our models in ways similar to those outlined in this study we can reduce the uncertainty of our future predictions, especially

on local scales, and with this improved knowledge we can plan for the future

References

Alpert, P., Krichak, S., Shafir, H., Haim, D. & Osetinsky, I. (2008), 'Climatic trends to extremes employing regional modeling and stastical interpretation over the eastern mediterranean', *Global Planetary Change* **63**.

Alpert, P., Stein, U. & Tsidulko, M. (2005), 'Role of sea fluxes and topography in eastern mediterranean cyclogenesis', *The Global atmosphere and ocean system* **3**(1), 55–79.

Evans, J. (2009), 'Global warming impact on the dominant precipitation processes in the middle east', *Theoretical and Applied Climatology, in press*. .

GoogleEarth (2009). // /.

Halpert, M. & Ropelewski, C. (1992), 'Surface temperature patterns associ-

Murphy, A. & Epstein, E. (1989), ‘Skill scores and correlation coe cients in model verification’, *Monthly Weather Review* **117**, 572–581.

NASA Goddard Space Flight Center (2009), ‘Global precipitation analysis’. [illegible] s[illegible] n s /.

Olson, D. & Dinerstein, E. (2002), ‘The global 200: Priority ecoregions for global conservation’, *Annals of the Missouri Botanical Garden* **89**, 199–224.

Partow, H. (2001), ‘The mesopotamian marshlands: Demise of an ecosystem’,

Wang, Y., Leung, L., McGregor, J., Lee, D.-K., Wang, W.-C., Ding, Y. & Kimura, F. (2004), 'Regional climate modeling: Progress, challenges and prospects', *Journal of the Meteorological Society of Japan* **82**(6), 1599–1628.